SMHI

Monthly Mean Cloud Cover per NWP Model

The impact of varying NWP background information on CM-SAF cloud products

Visiting Scientist Report
Climate Monitoring SAF (CM-SAF)

Matthieu Trolez, Karl-Göran Karlsson, Sheldon Johnston and Peter Albert

The impact of varying NWP background information on CM-SAF cloud products

Visiting Scientist Report
Climate Monitoring SAF (CM-SAF)

Matthieu Trolez, Karl-Göran Karlsson, Sheldon Johnston and Peter Albert

Report Summary / Rapportsammanfattning

Author (s)/Författare

Matthieu Trolez, Karl-Göran Karlsson, Sheldon Johnston and Peter Albert

Title (and Subtitle/Titel)

The impact of varying NWP background information on CM-SAF cloud products

Abstract/Sammandrag

The purpose of this study was to quantify the impact of using ancillary data from Numerical Weather Prediction (NWP) models in the derivation of cloud parameters from satellite data in the Climate Monitoring Satellite Application Facility (CM-SAF) project. In particular, the sensitivity to the NWP-analysed surface temperature parameter was studied.

A one-year dataset of satellite images over the Scandinavian region from the Advanced Very High Resolution Radiometer (AVHRR) on the polar orbiting NOAA satellites was studied. Cloud products were generated by use of the Polar Platform System (PPS) cloud software and the sensitivity to perturbations of the NWP-analysed surface temperature was investigated. In addition, a study on the importance of the chosen NWP model was also included. Results based on three different NWP models (ECMWF, HIRLAM and GME) were analysed.

It was concluded that the NWP model influence on the results appears to be small. An interchange of NWP model analysis input data to the PPS cloud processing method did only lead to marginal changes of the resulting CM-SAF cloud products. Thus, the current CM-SAF cloud algorithms produce robust results that are not heavily dependent on NWP model background information.

Nevertheless, the study demonstrated a natural high sensitivity to the NWP-analysed surface skin temperature. This parameter is crucial for the *a priori* determination of the thresholds used for the infrared cloud tests of the PPS method. It was shown that a perturbation of the surface skin temperature of one K generally resulted in a change of cloud cover of about 0.5-1 % in absolute cloud amount units. However, if perturbations were in the range 5-10 K the change in cloud cover increased to values between 1 to 2 % per degree, especially for positive perturbations. Important here is that a positive surface temperature perturbation always leads to an increase in the resulting cloud amounts and vice versa.

Key words/sök-, nyckelord

CM-SAF cloud products, PPS, NWP impact.

Table of content

1. Introduction

The original objective of this Visiting Scientist study for the Climate Monitoring Satellite Application Facility (CM-SAF) project was the following:

- To quantify the impact of data from Numerical Weather Prediction (NWP) models on cloud parameters derived from satellite data.

In particular, the study should

a) cover an analysis of small-scale surface temperature variation at satellite resolution and its influence on cloud fractional cover,
b) conduct a sensitivity analysis of vertical profile information (e.g., temperature, pressure) on cloud-top parameters (e.g., cloud-top height, pressure, temperature) and
c) quantify the error budget of cloud parameters with respect to changes of the surface temperature and different profile data.

Cloud macrophysical products, such as cloud coverage and cloud-top height/pressure/temperature can be inferred from satellite imagery (i.e., from level 1b radiance data) if the atmospheric state is known, at least to a certain extent. The operational chains for retrieving cloud information from AVHRR and MSG radiances make use of some background data from NWP models, i.e., typically the surface temperature, the vertical temperature profile and the vertically integrated atmospheric moisture content. The spatial resolution of NWP model data is, however, poor if compared against common high resolution satellite imagery and this could introduce a bias in the results. In addition, potential deficiencies in the parameterisation of boundary layer processes and surface fluxes (not being fully resolved by the model) of the NWP models could also affect results negatively. Consequently, it is very important to try to estimate how sensitive CM-SAF cloud retrieval methods are to the used background information. If also considering that one of the desired objectives of the CM-SAF is to provide independent validation datasets for NWP and climate models, it is clear that this task is critical for the credibility of CM-SAF climate datasets.

After some initial studies of the problem area it was felt that the scope for the study had to be reduced and more focused compared to what was stated in the original very ambitious study tasks. For example, it turned out to be very difficult to study the first aspect above (a) due to the lack of real ground truth observations with the required horizontal resolution. In addition, the option to use cloud-free infrared imagery to estimate surface temperatures and their local variation was in the end not considered as acceptable. The reason is that this would actually require absolute confidence in the satellite-derived cloud products (cloud masks) and that surface emissivity variations could be effectively compensated for. Due to remaining ambiguities here it was decided to instead focus on the two other tasks above (b and c).

Consequently, the following more specific and focused study tasks were formulated:

1. Estimate the impact on CM-SAF cloud mask, cloud type and cloud top products due to variations in the NWP-analysed surface temperature parameter. Use surface temperature data from one particular NWP model as a basis for the study and try to quantify the sensitivity to the surface temperature parameter. The analysis shall cover the atmospheric variability encountered during one entire year (i.e., all different seasons).
2. Define a common NWP dataset containing information from at least three NWP models: HIRLAM (High Resolution Limited Area model, used in the Scandinavian countries plus the Netherlands and

1

Spain), GME (German global Meteorolological model) and ECMWF (European Center for Medium Range Weather Forecasts). Compute some general statistics to get a preliminary overview of how the models compare for the crucial parameters (e.g. surface temperature).

3. Study the impact on CM-SAF cloud mask, cloud type and cloud top results due to the use of different NWP models (i.e., HIRLAM, GME and ECMWF as defined in the common model dataset).

Notice that task 3 is here a restricted way of solving the original task b) above. A more systematic and thorough solution to this task would require use of more sophisticated methods (e.g. making use of datasets produced by ensemble prediction systems- EPS) in order to cope with the very large amounts of data that would be generated when perturbing full atmospheric profiles. We have considered the latter approach as out of scope of this study but interesting enough for potential consideration later on in the future.

After giving some background information on available CM-SAF cloud processing schemes and NWP datasets in Section 2, all three tasks above are subsequently covered in Sections 3, 4 and 5. Conclusions and an outlook for the future are then finally given in Section 6.

2. Background

2.1 PPS cloud products

The cloud products studied here are the CM-SAF products generated from polar satellite imagery. The CM-SAF is using the Polar Platform System (PPS) cloud software developed by the Satellite Application Facility in support of Nowcasting (NWCSAF). PPS Cloud products are generated using data from the Advanced High Resolution Radiometer (AVHRR) onboard the National Oceanic and Atmospheric Administration (NOAA) satellites. Cloud processing uses several auxiliary data sources in addition to basic image radiances: land-sea masks, surface type information, surface topography information and data from NWP models. The NWP models used in this study were the:

- High Resolution Limited Area Model (HIRLAM), used at the Swedish Meteorological and Hydrological Institute (SMHI) for short range forecasting

- Global Modell Europa (GME) used at the German Weather Service (DWD)

- Global atmospheric model from the European Center for Medium range Weather Forecasts (ECMWF)

They are used to provide *a priori* estimates of the following atmospheric parameters:

- ❧ The column integrated water vapour content, surface (skin) temperature, and temperature at the 950 hPa level for the extraction of the PPS Cloud Mask product.

- ❧ In addition to these, the 850 hPa, 700 hPa, 500 hPa, and tropopause level temperatures are needed for the extraction of the PPS Cloud Type product.

- ❧ The temperature and specific humidity at the highest possible vertical resolution (available model levels) are needed for the retrieval of the PPS Cloud Top products.

For each satellite scene, cloudy pixels are identified and classified by comparing different features of the satellite images and NWP data to grouped sets of thresholds. In this study, we focused on the use of

the **T11T$_{SFC}$** feature. This feature is the difference between the measured brightness temperature at 11 μm (AVHRR channel 4) and the assumed surface skin temperature (as provided by the NWP model).

The PPS Cloud Mask (CM) product is generated using sequences of generic tests. Pixels are classified into four categories: cloud free, cloud contaminated, cloud filled, and snow/ice contaminated. The composition of each sequence depends on the environmental regime, i.e., illumination conditions and surface type, of the pixel considered. Each generic test contains a group of threshold tests for various image features. The **T11T$_{SFC}$** temperature difference is present in several of these tests as well as in both the snow and the cloud screening processes. Table 1 lists the different generic tests involving this feature. When studying how the components listed are actually used in these sequences, two important characteristics of this feature are revealed:

   ɔ   It is used in all the environmental regimes considered

   ɔ   It is one of the first features to be tested (except in case of low-level temperature inversion). This is important because, when a sequence is tested, it is halted at the first successful generic test (satisfying a quality margin). Consequently this feature is important for the output of the CM as it is almost always tested.

Table 1. *A list of the generic tests involving the T11TSFC feature.*

Snow screening process	Cloud screening process
Snow/Ice Sea	Cold Cloud
Snow Land (if no temp. inversion)	Cold Water Cloud
Snow Mountain	Thin Cold Cirrus
Snow Twilight (if no temp. inversion)	Cold Bright Cloud
	Cloud in Sunglint
	Cold Clouds in Sunglint

During the generation of the PPS Cloud Type (CT) product, the cloudy pixels (according to the CM product) are first put into two larger categories: opaque and semi-transparent/fractional clouds. New sequences of threshold tests are performed to further sub-divide the semi-transparent/fractional cloud group into more specific cloud types. These tests are primarily based on the **T11T12** feature (i.e., brightness temperature differences between AVHRR channels 4 and 5 at 11 and 12 microns). For the opaque group of clouds, the **T11T$_{SFC}$** feature (except for the elevated terrain) is used for a further separation into low- mid- and high-level cloud types. Consequently, the **T11T$_{SFC}$** feature is likely to have a great impact on the output for both the Cloud Mask and the Cloud Type.

The Cloud Top Temperature and Height (CTTH) product is retrieved for each cloudy pixel following two distinct processes, depending on their cloud type. The temperature at the top of semi-transparent clouds is retrieved using a histogram technique. This technique utilizes the brightness temperature differences of AVHRR channel 4 and 5 as caused by different cloud transmissivities in the two channels for thin clouds (Korpela et al, 2001). The pressure at the top of opaque clouds is retrieved by simulating the cloudy and cloud free top of the atmosphere (TOA) radiances, acquired from the radiative transfer model RTTOV (Saunders et al., 1999) and NWP data, and comparing them with the AVHRR channel four temperatures.

More details on the derivation of the cloud products are given by Dybbroe et al. (2005a and 2005b) and NWCSAF SUM (2008).

2.2 NWP models

Three models were chosen for this study. These are HIRLAM (Swedish version used at SMHI), GME (from the German weather service DWD), and the atmospheric model from the European Center for Medium Range Weather Forecasts (ECMWF). While GME and ECMWF are global models, the HIRLAM model is run only over a limited area. Table 2 gives the valid resolution of each model for the specific model versions used in this study. An analysis of the degree of agreement of the different models over the period of this study (August 2004 - July 2005) is presented later in section 4. Not much more will be said about each model as this lies outside the scope of this study. It should however be noted that, because the development of PPS has been based on the use of the HIRLAM model, PPS is tuned to this model. One can consequently expect more realistic results in the Cloud Products when HIRLAM is used. For more details about these models visit:

GME: http://www.dwd.de/de/FundE/Analyse/Modellierung/model.htm

ECMWF: http://www.ecmwf.int/products/forecasts/guide/The_ECMWF_global_atmospheric_model.html

HIRLAM: [Undén et al., 2002]

Table 2. *Spatial resolution of the different NWP models used. The value given in km is latitude dependent and is consequently an average value, computed over the center of the **Baltrad1km** area (see Figure 1).*

NWP model	Grid Resolution	Resolution (km)
HIRLAM	0.2^o x 0.2^o	≈ 22
GME	0.5^o x 0.5^o	≈ 55
ECMWF	0.5^o x 0.5^o	≈ 55

3. Sensitivity Study

This part of the study analysed the changes in PPS Cloud Products resulting from a constant bias in the NWP surface temperature field. A statistical analysis was performed on a set of Cloud Products, obtained by processing each satellite scene several times with a different bias in the surface temperature.

3.1 Data

The dataset used, named Year-Wide biased dataset (YWb), ranged from June 2004 to May 2005.

Satellite scenes from NOAA-16 and NOAA-17 were selected by applying a sampling (described in Table 3), to the NOAA data archive available at SMHI. This sampling made the datasets as equally distributed (with respect to date, time, and satellite) as possible. Four unavailable dates (due to missing raw satellite data) were slightly shifted in time (±2 days) and five dates were unavailable. As a result, the YWb dataset contain 66 scenes.

Table 3. *Sampling schedule used to create the Year-Wide datasets.*

Day of the month	Satellite	Hour[1]
1st	NOAA16	Day
6th	NOAA17	Day
11th	NOAA16	Night
16th	NOAA17	Night
21st	NOAA16	Day
26th	NOAA17	Day

Subsequently, PPS cloud products (Cloud Mask, Cloud Type, and Cloud Top Temperature and Height) were generated on the ***Baltrad1km***[2] area for this set of scenes. For each satellite scene, seven runs were performed, each one with a bias, chosen in the range {0 K, ±1 K, ±5 K, ±10 K}, in the surface temperature field. For each pixel the following equation was applied:

$$NWP_{sfctemp_{used}} = NWP_{sfctemp_{model}} + bias \qquad (1)$$

where $NWP_{SFCtemp_{used}}$ is the surface temperature estimate used in the PPS processing, $NWP_{SFCtemp_{model}}$ is the surface temperature given by the HIRLAM model, and *bias* is the constant bias in the bias range data set {0 K, ±1 K, ±5 K, ±10 K}.

Consequently, the YWb dataset comprised seven sets of cloud products (each one containing results from 66 AVHRR scenes) generated with modified NWP data from the HIRLAM model.

3.2 Analysis method

The different sets of cloud products in the YWb dataset were analysed in a statistical way in order to extract relevant figures for each cloud product. The studied quantities were the area mean cloud cover (or cloud amount) derived from the cloud mask product and the distributions of cloud types and cloud heights.

The sensitivity of the cloud mask product to the biases in the surface temperature field was estimated by studying the area mean cloud cover, as defined in Equation 2.

$$\langle Cloud\ Cover \rangle = \frac{Number\ of\ cloudy\ pixels}{Total\ number\ of\ processed\ pixels} \qquad (2)$$

The average cloudiness of each scene was calculated over the ***Baltrad1km*** area (Figure 1). This area is

---

[1]"Day" refers to the overpass closest to noon and "Night" to the one closest to midnight.
[2] The ***Baltrad1km*** area extends from the Norwegian Sea to western Russia and down to central Germany (Figure 1).
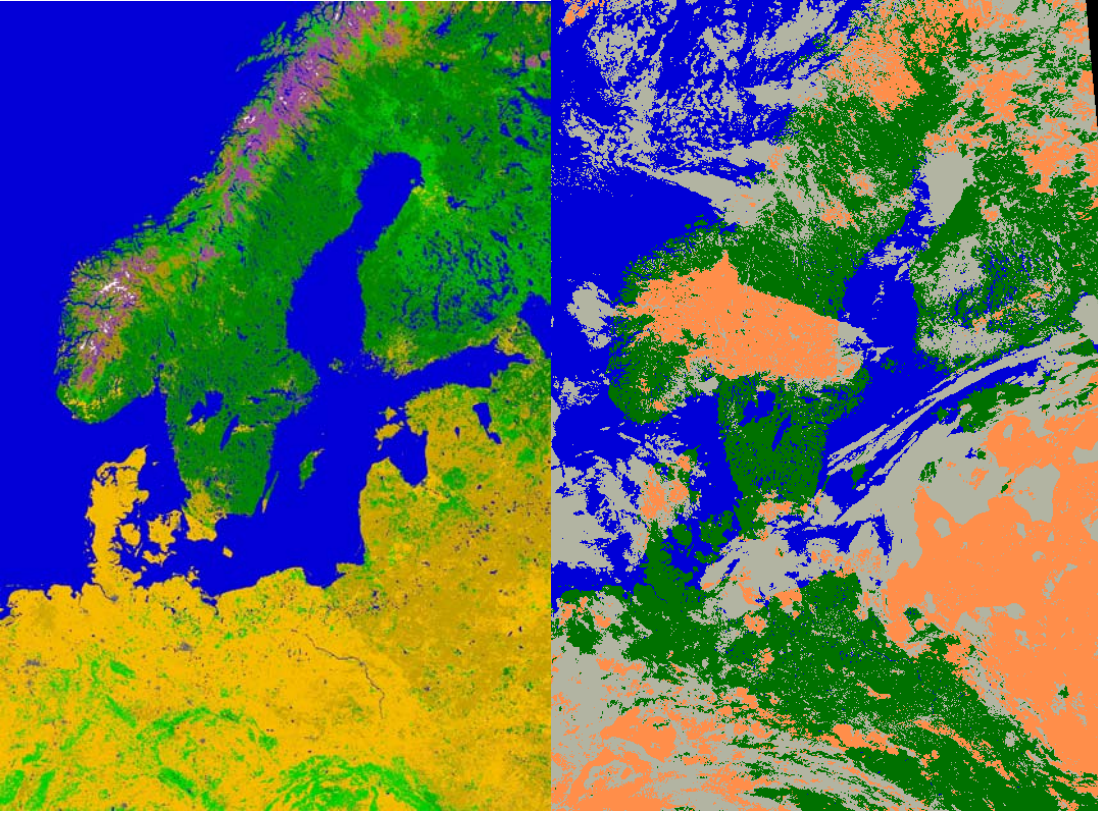
5

Figure 1. *Overview of the **Baltrad1km** area (**left**, colours corresponding to different USGS land use categories) and a corresponding PPS Cloud mask product (**right**, opaque clouds in orange and thin clouds in grey) over this area from April 16 2005 at 20:52 UTC.*

defined in Lambert Azimuthal Equal Area projection (true scale at 60°N latitude and true North-South direction at 0° longitude) with 1 km horizontal resolution. Results were then averaged over time, resulting in coarsely estimated monthly means (based on typically 6 values per month).

For further analysis of the sensitivity to surface temperature variations, we define parameter δ_α in Equation 3 below,

$$\delta_\alpha = \frac{\langle \text{Cloud Cover} \rangle_\alpha - \langle \text{Cloud Cover} \rangle_{ref}}{|\alpha|} \tag{3}$$

where *ref* is the reference run (*bias=0*) and α is the value of each bias considered. The δ_α parameter describes the average change in cloud cover per degree surface temperature bias.

3.3 Results for the area averaged cloud amount

Figure 2 shows the resulting time-series of monthly mean cloudiness[1] over the **Baltrad1km** area. Each

---

[1] Observe that this value **does not in any way** represent a true monthly mean since it is only based on 4-6 observations!

line and associated symbol corresponds to a different value of the bias.

What can be easily seen from Figure 2 is that the cloud cover increases with a positive surface temperature perturbation while it decreases with a negative perturbation. We can understand this by considering the following:

- The PPS **T11T**$_{SFC}$ test checks if the **T11T**$_{SFC}$ temperature difference exceeds a prescribed value ∆**T** computed as the sum of an atmospheric correction value plus a static threshold offset (typically 7 K over ocean surfaces). If this difference is exceeded (i.e., the **T11** measurement is at least ∆**T colder** than the surface), the pixel is declared cloudy.

Notice that the mentioned threshold offset value is a tuneable parameter used to compensate for atmospheric influences and for typical errors in the NWP estimation of the surface (skin) temperature parameter. In that sense, ∆**T** should be seen as a kind of safety margin for the cloud detection process.

With this background, it should be clear that the effect of adding a negative perturbation to the surface temperature is equivalent to increasing the safety margin. In other words, detected clouds are here further prevented from being mistaken for clear surface pixels. This also means that near-surface clouds (which normally are not very frequent) will no longer be detected, thus the total cloud amount decreases but only relatively modestly. As a contrast, the adding of a positive perturbation will be equivalent to decreasing the safety margin. In particular, adding a perturbation as large as 10 K (which is larger than the typically used threshold offset values) means in practice that the safety margin is completely removed. The consequence is that a considerable amount of truly cloud-free pixels are now misclassified as being cloudy. This explains why a positive perturbation (i.e., curves for +1 K, +5 K and +10 K) in Figure 2 gives a considerably larger deviation than the corresponding negative perturbation.

Deviations as a function of the perturbation or bias in Figure 2 seem fairly constant with respect to the time of year which means that the computed δ_α parameter values (as defined by Equation 3) are also quite stable over the seasons (Table 4). The only exception is seen during winter when deviations for the negative perturbations are somewhat larger than for other seasons. We notice that the change of cloud cover per degree of surface temperature perturbation is generally well beneath 1 % for negative perturbations while the change for positive perturbations are generally higher than 1 %. In particular, the value increases for higher absolute perturbations (e.g., exceeding 2 % for δ_{+10} in summer and in spring). Thus, we conclude that PPS cloud results are significantly more sensitive to positive surface temperature biases than to negative biases. Furthermore, sensitivities increase for the positive case with the value of the bias. This is a natural consequence of the influence of the temperature perturbation for the used safety margins according to the discussion earlier on this page.
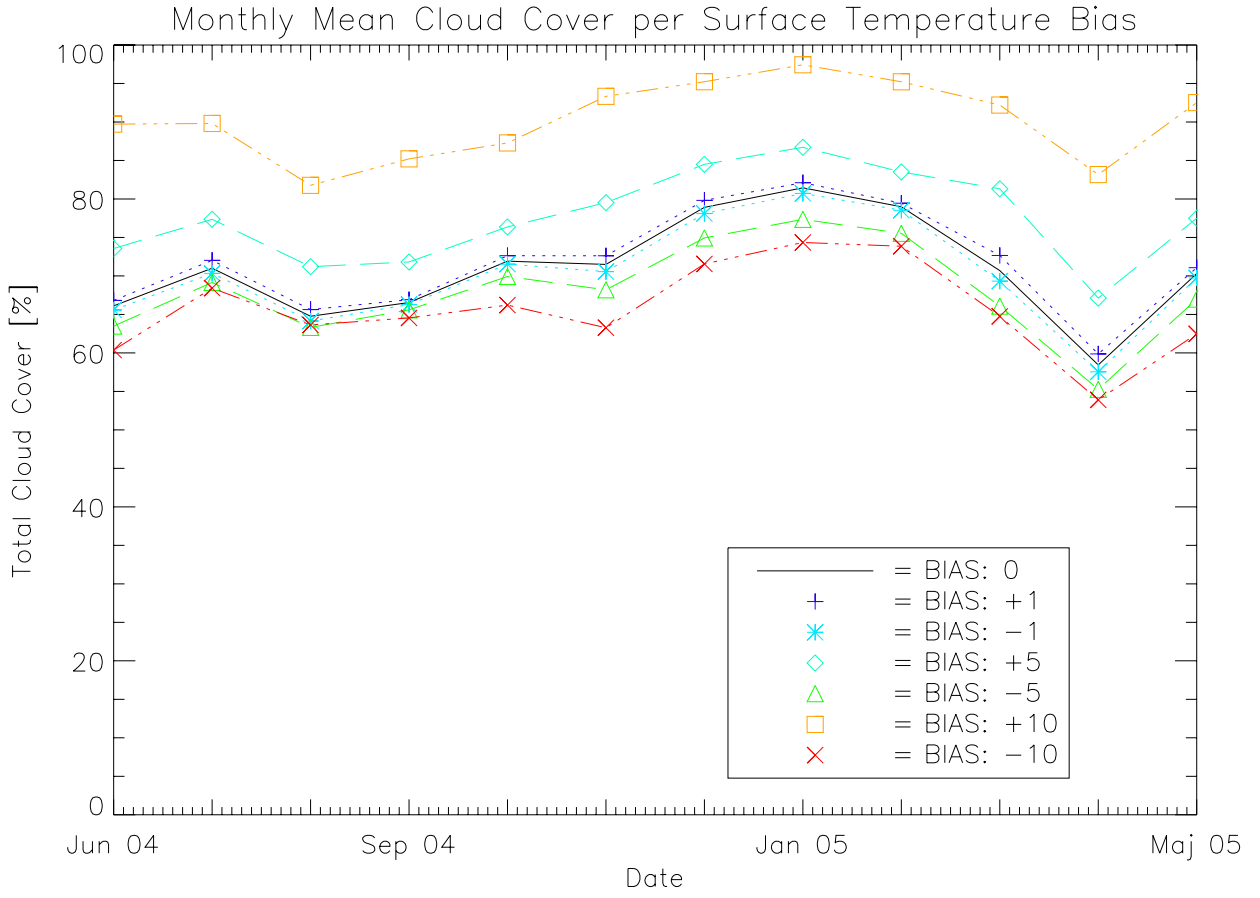
Figure 2. *Time-series of monthly mean cloud cover for each value of the surface temperature perturbation (bias).*

Table 4. *Change in cloud cover per degree change in the NWP surface temperature. The definition of δ is given by equation 4. Notice that the first month of summer is June.*

Bias	Summer	Fall	Winter	Spring
δ_{-10}	-0.57%	-0.20%	-0.73%	-0.59%
δ_{-5}	-0.52%	-0.19%	-0.79%	-0.92%
δ_{-1}	-0.53%	-0.26%	-0.80%	-1.37%
δ_{+1}	+0.71%	+0.37%	+0.91%	+1.96%
δ_{+5}	+1.49%	+1.05%	+1.12%	+2.12%
δ_{+10}	+2.36%	+1.87%	+1.63%	+2.15%

8

3.4 Results for the area averaged frequency distribution of cloud types

To evaluate the sensitivity of the Cloud Type product to the introduced surface temperature perturbations, four different sub-categories of clouds were defined:

- ✧ "**Low clouds**" (*regrouping of PPS cloud types no. 6 and no. 8*)
- ✧ "**Medium clouds**" (*PPS cloud type no. 10)*
- ✧ "**High opaque clouds**" (*regrouping of PPS cloud types no. 12 and no. 14*)
- ✧ "**High semi-transparent clouds**" (*regrouping of PPS cloud types nos. 15-18*)
- ✧ "**Fractional clouds**" (*PPS cloud type no. 19)*

Figure 3 shows incremental and accumulated contributions to the total area mean cloud cover (given by the top curve denoted Fractional) from these sub-groups of clouds as a function of surface temperature perturbation (bias) value. Results are computed from all 66 utilised AVHRR scenes. The resulting values of total cloud amount differ slightly from what can be deduced from Figure 2 but these differences are rather small and due to rounding errors affecting exclusively results in Figure 2.

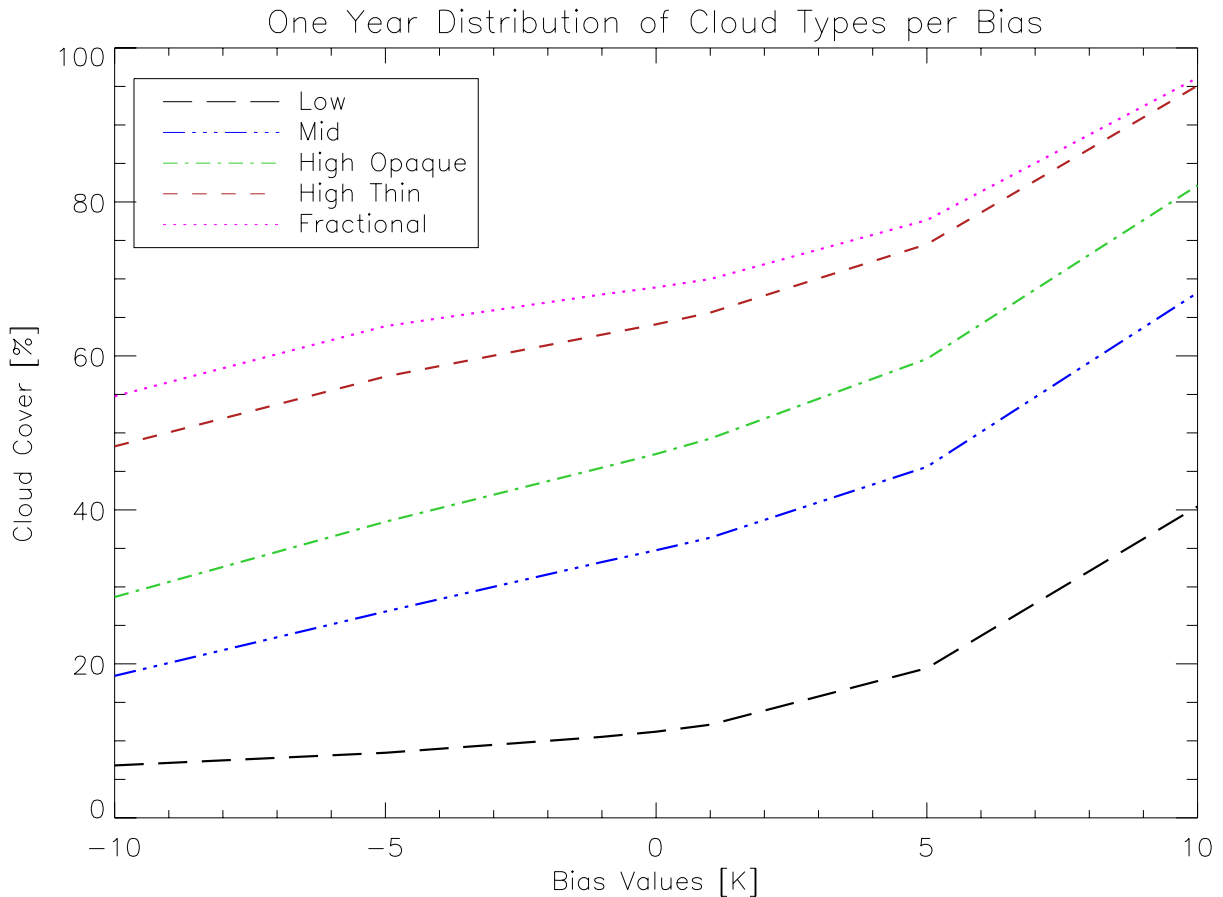**Figure 3.** *Accumulated contributions to the total area mean cloud cover from five sub-groups of clouds as a function of surface temperature perturbation (bias) value. Notice that curves show contributions that are subsequently added; first for Low, then added in the order Mid, High Opaque, High Thin and Fractional, which means that the curve for Fractional shows the final total area mean cloud cover.*

Figure 3 shows in an alternative way how positive bias perturbations are more serious than negative bias perturbations for cloud amount results (i.e., creating increasing slopes for all contributions). Furthermore, the figure clearly shows the greatly increasing contributions from the Low cloud category for positive biases, indicating an increasing misinterpretation of clear surface pixels as low-level clouds. It is interesting to notice that nearly 40 % of all clouds for the bias value +10 K are classified as Low compared to only about 10 % for the unperturbed case.

For the negative perturbations we notice that clouds are lost mainly from the Mid category and not so much from the presumed Low category. This indicates that a large part of the Low-level clouds are actually detected by image feature tests (e.g. reflectance tests) that do not involve the use of the **T11T$_{SFC}$** image feature and at some point this means that a further increase of the safety margin (i.e., applying larger negative perturbations) does not mean so much. But, instead we now begin go loose clouds from the Mid-level clouds groups since the safety margin reaches as much as 17 K for the largest perturbation (i.e., negative bias of 10 K plus the standard threshold offset which is typically 7 K).

Figure 3 also gives interesting information concerning the contribution from Fractional clouds and partly also from high thin (semi-transparent) clouds. It appears as the contribution from these cloud groups decreases when going from negative to positive perturbations. The most reasonable explanation is that this is caused by the use of varying atmospheric corrections when defining PPS thresholds for the **T37T12** and **T11T12** brightness temperature difference features. In a situation with simulated warmer surface temperatures, a larger atmospheric correction is implied (i.e., more radiation can be absorbed by atmospheric constituents) which means that a diminishing remaining part of the truly measured brightness temperature differences could be interpreted as a sign of the presence of fractional or semi-transparent clouds. Thus, in the case of overestimated surface temperatures we would risk missing fractional and semi-transparent clouds due to their dependence on detectable and significant **T37T12** and **T11T12** brightness temperature differences.

3.5 Results for the area averaged frequency distribution of cloud top heights

Finally, we will now study the sensitivity of the Cloud Top Height product to the introduced surface temperature perturbations. Figure 4 shows the absolute frequency (i.e., number of pixels) of cloud top height categories in bins of 500 m vertical resolution as a function of surface temperature perturbation value. The frequencies are computed from the entire studied dataset, i.e. from all analysed 66 AVHRR scenes.

We notice that in the unperturbed case (bias=0) there is a maximum in cloud occurrence for cloud heights between 2 and 3.5 km. Above this layer, frequencies are quite stable and about the same all the way up to approximately 10 km's height. Above this height values decrease rapidly. Again, we see a more drastic change of the distributions for positive perturbations compared to the case for negative perturbations. As already indicated earlier for the cloud type product, frequencies of mid-level clouds decrease slightly for negative perturbations but values are otherwise quite stable. As a contrast, frequencies of low and mid-level clouds (i.e., below 4 km height) increase drastically for positive perturbations. For high-level clouds changes are rather small but some reduced frequency for the highest cloud heights are observed. This is consistent with the corresponding small decrease of the contribution from Fractional and High Thin clouds which was seen previously for the Cloud Type product.
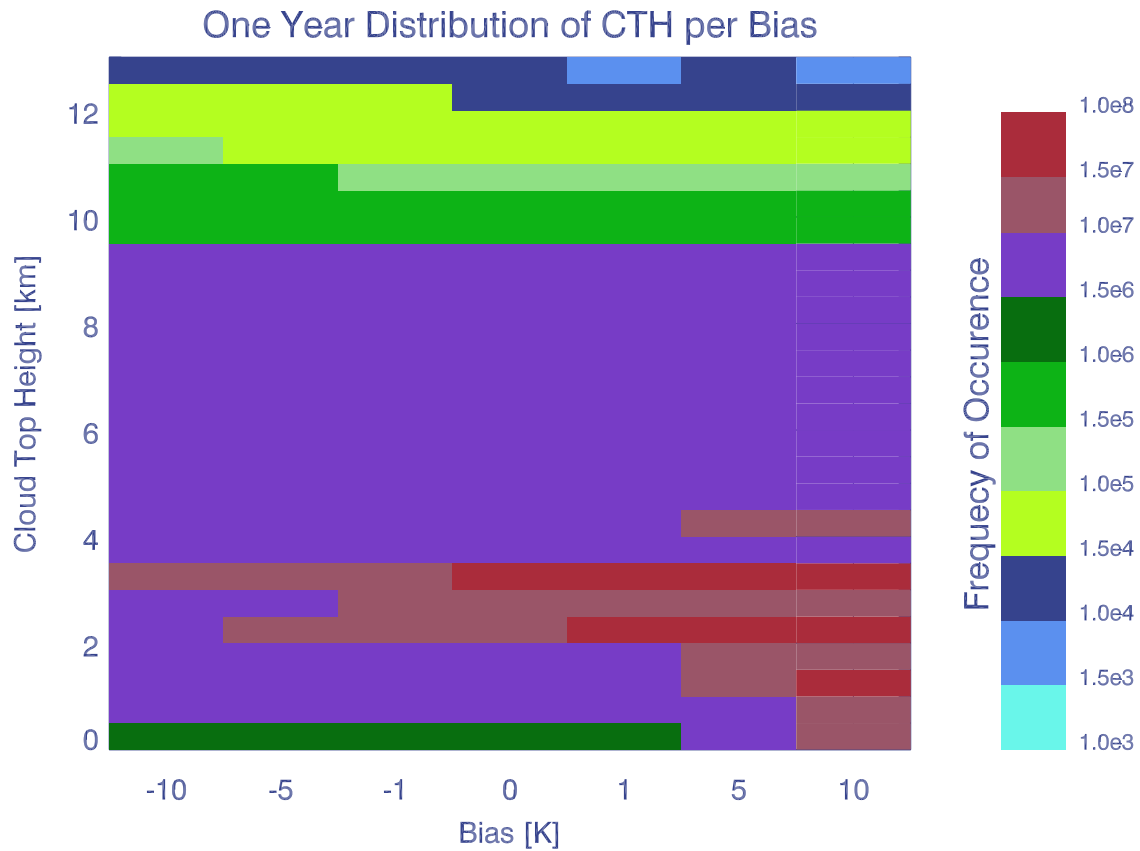
Figure 4. *Absolute frequency (i.e., number of pixels) of cloud top height categories (in bins of 500 m vertical resolution) as a function of surface temperature perturbation (bias) value.*

4. Preparing the PPS NWP model inter-comparison study: Analysis of initial model differences

In this section we will present some basic results from a statistical analysis of the surface temperature fields provided from three different NWP models that were chosen for the inter-comparison: HIRLAM, GME and ECMWF. The primary intention is to try to identify if there are general and typical differences between the model results that we can identify prior to providing them as input to PPS processing. Secondly, we hope that we later in section 5 can utilise the results together with conclusions from the previous section to understand the impact of these differences on the final PPS results.

4.1 Data and method

The available data consisted of individual differences for each grid point and each NWP model analysis, summing up to a considerably large dataset. Therefore, heavy averaging was necessary. Regardless of the common grid used, the data was processed as follows: First all individual NWP fields were interpolated to the common grid. For each grid point a time series of differences was then available for each model combination. For each month, those time series were first averaged in time,

which produced fields of (temporal) bias and standard deviation. Example fields of calculated bias and standard deviation are shown in Figure 6. for May 2005. The monthly fields of bias and standard deviation were calculated for each month, all grid points and all three possible model combinations. In a second step, both fields were now spatially averaged for each month. This leads to confusing values like standard deviations of standard deviations, therefore the finally studied monthly mean values are summarised below in Table 4 together with a short description:

Table 5. *Monthly mean quantities (left column) and their explanation (right).*

Mean bias	**Spatial average over individual mean temporal differences at each grid point**
Standard deviation of bias	**Spatial variability of individual mean temporal differences at each grid point**
Mean standard deviation	**Spatial average over individual temporal standard deviations at each grid point**
Standard deviation of standard deviation	**Spatial variability over individual temporal standard deviations at each grid point**

Three different NWP analysis datasets have been investigated in terms of differences between their surface temperature, namely data from the ECMWF's global atmospheric model, HIRLAM (SMHI implementation) and GME (DWD implementation). HIRLAM is a regional model (model domain indicated in Figure 6) while the others are global models.

In addition to the different regional coverage, the different spatial resolution has also to be taken into account. The HIRLAM model is a grid point model which was operating on a rotated grid with approximately 0.2° (20 km) resolution for this study. The ECMWF model is a spectral model with physical quantities defined in a Gaussian grid. The used version had a horizontal resolution of approximately 0.5° (50 km). The GME model results are originally defined on an icosaeder grid. For this CM-SAF study, results were transformed to a regular non-rotated grid with 0.5° (50 km) resolution.

Before the three datasets could be compared they had to be transformed onto a common grid. In the presented work all NWP datasets were interpolated to a given set of latitude / longitude pairs. In the case of ECMWF and HIRLAM this was achieved by transforming the latitude / longitude pairs into model grid indices, the interpolation was then performed in grid space. In case of GME, the interpolation was directly performed in latitude / longitude space.

Two different common grids have been used: In a first step the complete initial CM-SAF Baseline area was coarsely covered by a regular grid with 1° resolution, ranging from 60°W to 60°E and from 30°N to 80°N, respectively. In a second step the original pixels of several sub regions, previously defined for the processing of AVHRR data using the PPS software, were used in order to more closely observe the possible implications on the cloud retrieval schemes in full satellite image resolution. The Baseline area, as covered by HIRLAM and ECMWF results, and the sub-regions are illustrated in Figure 6.

The datasets available for this investigation cover a full year ranging from June 2004 to May 2005; however, the temporal resolution is relatively poor. The time interval between two consecutive analyses is 6 hours in all datasets, but not all possible dates and times were included. This is further illustrated in Figure 5 where each NWP analysis is marked with a dot.
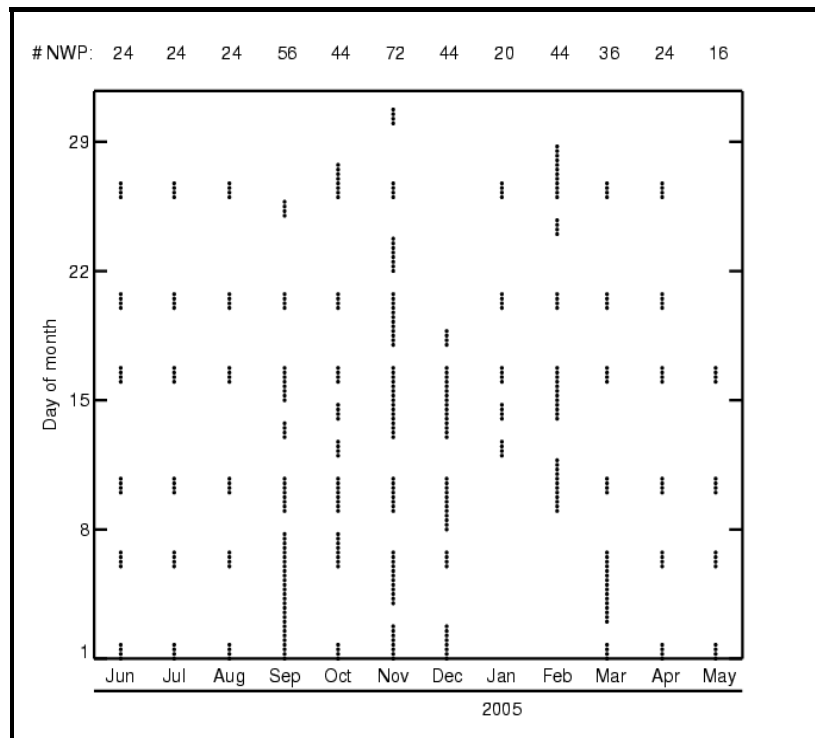
Figure 5. *Temporal coverage of the NWP datasets available for this work. Each dot represents one NWP analysis. The numbers on top give the total number of datasets per month (out of possible 124).*
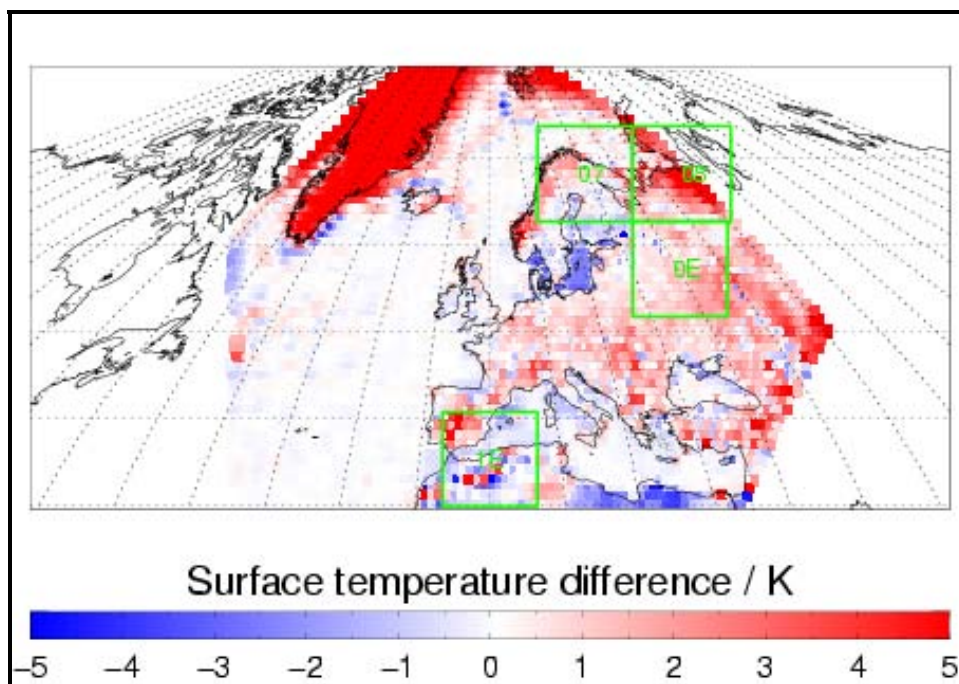

Figure 6. *Monthly bias of surface temperature between the HIRLAM and ECMWF NWP analyses, calculated on a 1° resolution. Data shown is for May 2005. The green squares show the sub-regions used for further studies in satellite resolution.*
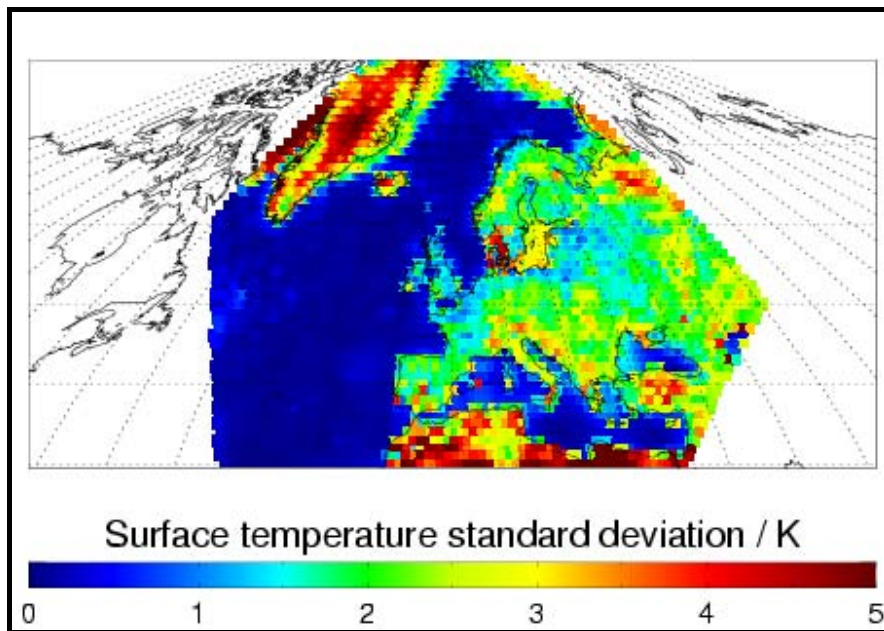
Figure 7. *Monthly standard deviation of surface temperature difference between the HIRLAM and ECMWF NWP analysis, calculated on a 1° grid resolution. Data shown is for May 2005.*

4.2 Results

Figure 8 summarises the results for the initial baseline area on the 1° grid. The upper panel shows the resulting mean differences, the lower panel the resulting mean standard deviations. The left figures each show the results for land and sea, the right figures show the results for land only. Some distinct features can be observed in all figures:

- The differences over land significantly exceed the differences over sea.

- The disagreement increases towards the end of the comparison period.

- The lowest differences occur between ECMWF and GME.

- Overall, handwavingly combining the different results, for any grid point the difference between the surface temperatures of two models can be expected to deviate up to 10 K with the majority of differences being between 1 and 7 K.

The corresponding results for the four individual tiles indicated in Figure 6 are presented in Figure 9. Only the resulting biases are shown. Increasing the spatial resolution of the comparison generally did not contradict the overall results for the complete Baseline area presented in Figure 8. However, it is well visible that e.g. the results for North Africa and southern Spain (tile 1E) do not show the bias increase towards the end of the comparison period. It is also visible that the variability of deviations differs from region to region. We have reason to believe that those differences are related to model differences in the treatment of snow cover and the snow melting period in spring which definitely would affect also the evolution of surface skin temperatures.

However, the main motivation for this study was not an in-depth investigation of model differences and their reasons but rather an investigation about which differences have to be expected when using one model or the other as input to the PPS software.

14

Combining the results for the initial Baseline area and the individual tiles, a sensitivity study varying the surface temperature about ± 10 K seems appropriate in order to estimate the possible effects from such a model change on the derived results. However, it is also clear that if studying larger regions and not only individual PPS processing tiles the average differences between models are normally only a few degrees. Thus, if referring to the results and conclusions of Section 3, we should consequently not see very large differences between area-averaged results over the studied Baltrad1km area unless also other differences between model states (e.g. as seen in full vertical moisture and temperature profiles) are present.
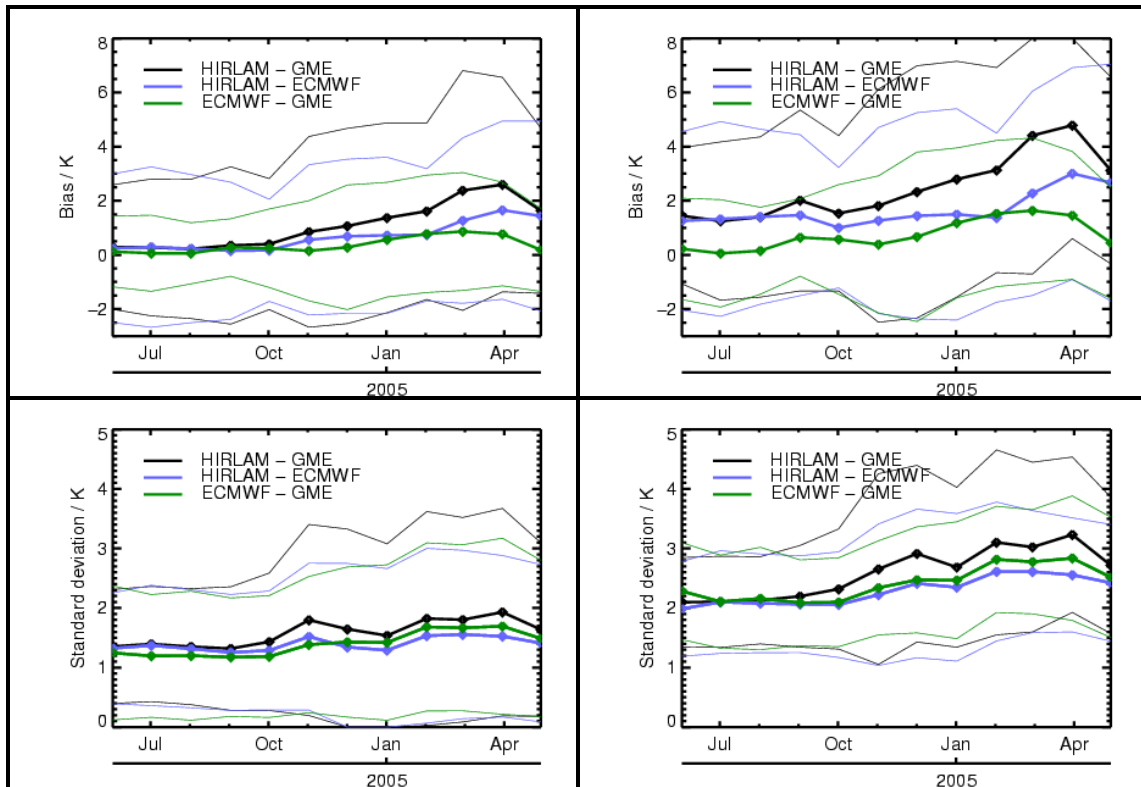
Upper left: mean bias land and sea	Upper right: mean bias land only
Lower left: mean standard deviation land and sea	**Lower right: mean standard deviation land only**

Figure 8. *Monthly mean and standard deviation of surface temperature difference between the three different models, calculated on a 1° resolution for the initial Baseline area. The thick lines each show the spatial averages of bias or standard deviations, the thin lines indicate the range given by ± the appropriate spatial standard deviations.*
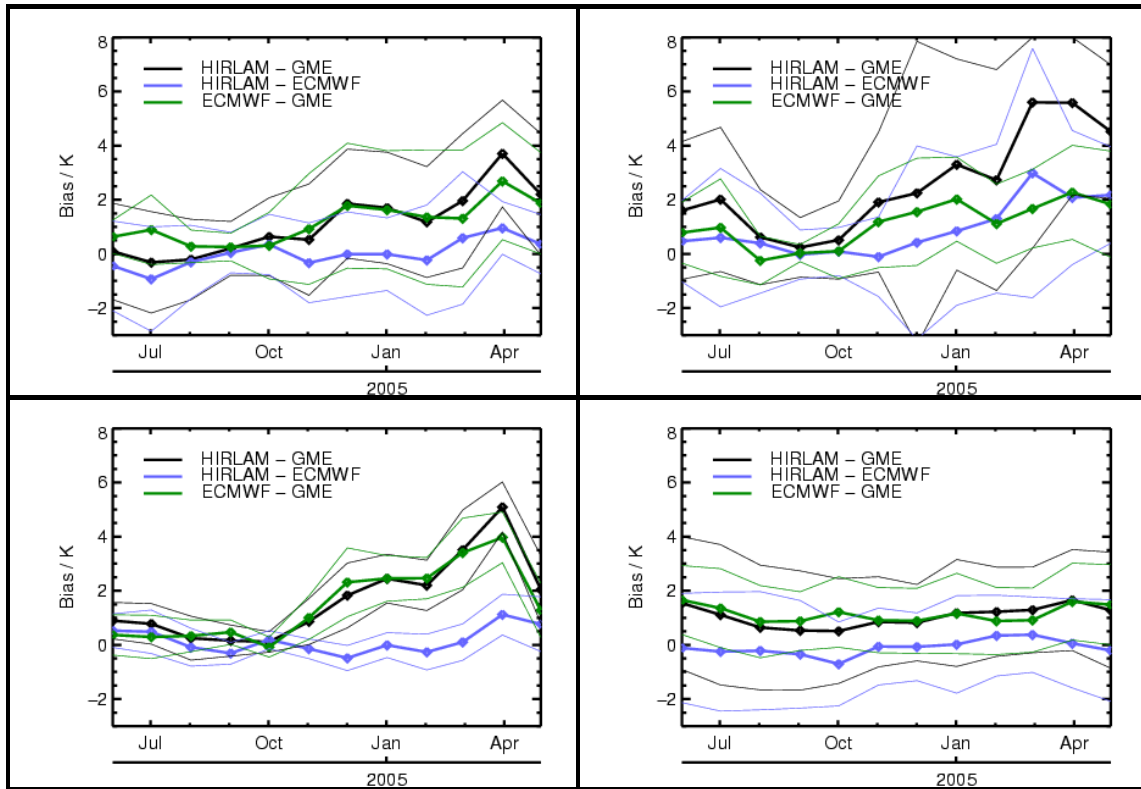
Upper left: tile 07   **Upper right: tile 08**
Lower left: tile 0E   **Lower right: tile 1E**

Figure 9. *Monthly mean surface temperature difference between the three different models, calculated on the sinusoidal projection with 1 km resolution used within the PPS processing. The thick lines each show the spatial averages of biases; the thin lines indicate the range given by ± the appropriate spatial standard deviations. The four panels show the results from four different tiles, the location of which is shown in Figure 6.*

5. Model effects on PPS cloud products

The last part of this study consisted of a direct comparison of the cloud products obtained with strictly the same input except for the background information from the NWP model which was varied.

5.1 Data

The same set of 66 NOAA AVHRR scenes, covering a whole year and prepared over the Baltrad1km area (Figure 1), was selected as in the sensitivity study described earlier in Section 3. However, the PPS results were now organised according to background NWP models instead of according to surface temperature perturbations. Table 6 summarizes the main similarities and differences between the previous sensitivity study dataset (named *Year-Wide biased*) and the current model study dataset (named *Year-Wide models*).

Table 8. *Similarities and differences between the two Year-Wide datasets.*

Year-Wide *biased* dataset	Year-Wide *models* datasets
Extends from June 2004 to May 2005	
Based on a set of 66 AVHRR scenes received by the Norrköping HRPT station	
Consists in several sets of PPS cloud products: CM, CT, CTTH	
7 sets: each created by inserting a bias in the NWP (HIRLAM) surface temperature field	3 sets: each created by using data from each NWP model (HIRLAM, ECMWF,GME)

5.2 Results for the area averaged cloud amount

The sensitivity of the Cloud Mask results to varying NWP model input was analysed by extracting the cloud cover (according to the previous Equation 2) for each set of data. The area averaged results are presented in Figure 10.

Results show a striking agreement between the three models. Differences appear to be very small. If comparing to the previous sensitivity study results in Figure 2 the deviations seen here appear comparable to a corresponding surface temperature difference of about 1-2 degrees. This is quite consistent with what was seen for the general differences (i.e., total area average) between models in Figures 8 and 9.

In order to conclude if the visible differences are exclusively explained by existing surface temperature differences and not by other factors (like differences in vertical profiles of temperature and humidity) we can try to analyse results in Figure 10 a little deeper. We notice that we can roughly describe the deviations in Figure 10 by the following periodic deviations:

Deviation 1 Jun-Jul 2004: ECMWF results slightly higher (1-2 %) than the other two

Deviation 2 Sep 2004:HIRLAM results slightly lower (1-2 %) than the other two

Deviation 3 Jan-Feb 2005: GME results slightly lower (about 1 %) than the other two

Deviation 4 Mar-Apr 2005: GME results lower (3-4 %) than the other two

When comparing with results of Figures 8 and 9 it is clear that three out of four of these deviations (Deviation 2 excluded) are definitely linked to the same kind of surface temperature deviations and associated cloud amount changes as was seen previously in Section 3. Especially for Deviation 4 it is very clear that GME mean surface temperatures are 1-4 K colder than both ECMWF and HIRLAM surface temperatures which is associated (as demonstrated in Section 3) with lower cloud amounts of the same order (in terms of percentage). We are tempted to conclude that deviations larger than 1-2 % are primarily linked to deviations in the models analysed surface temperatures. Smaller deviations could be attributed to variations in the vertical profiles of moisture and temperature.

A final comment here is that even if the area averaged results do not differ much we could still imagine finding regions where deviations are considerably larger. For example, Figures 6 and 7 indicate that there are certain regions where models more frequently disagree (local large biases associated with high standard deviations) than in other regions. In that sense, the choice of NWP model could still be critical.
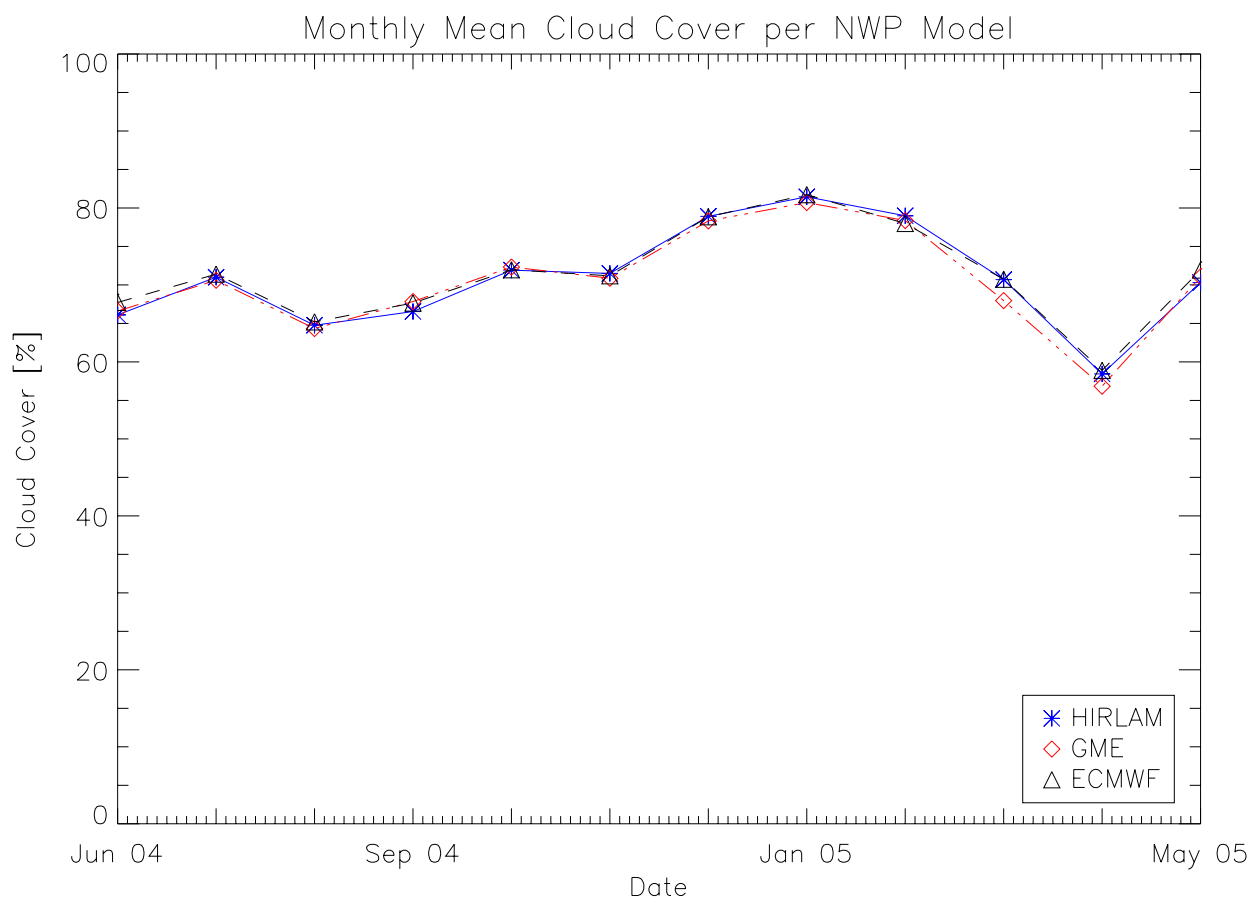
Figure 10. *Time-series of PPS-derived monthly mean cloud cover over the Baltrad1km are for each NWP model used as background information for the PPS cloud software.*

5.3 Results for the area averaged cloud type distribution

Figure 11 shows the corresponding results for the average cloud type distribution. The same set of cloud type categories was used as in the previous section 3.4.

As a consequence of the results in Figure 10 (small differences), we notice that the annual average total cloud amount (i.e., the total height of columns in Figure 11) is practically the same for all three models. Moreover, we can see that the contributions from the cloud type categories are also more or less the same. Thus, we conclude that the models ability to provide general atmospheric conditions with the details required for PPS processing appear to be quite similar for all three models. Existing differences do not seem to affect PPS results in a serious way.

5.4 Results for the area averaged frequency distribution of cloud top heights

It was decided not to further analyse and present corresponding results and differences for the cloud top height distribution. Results for the cloud type categories in the previous section showed already that also for cloud top heights the differences would be very small and even hardly distinguishable.
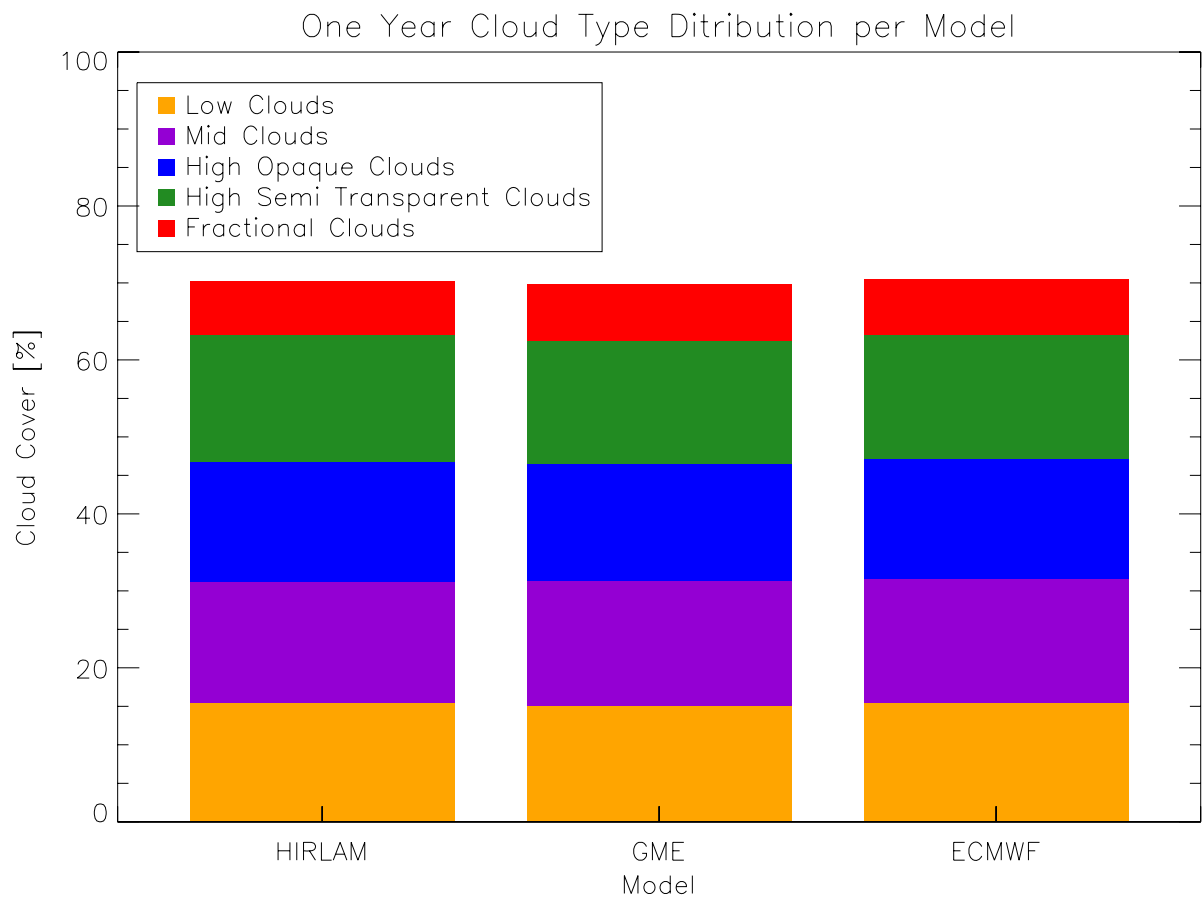
Figure 11. *Accumulated total contributions to the total cloud cover from five cloud type categories over the Baltrad1km in the period June 2004 to May 2005 for each NWP model.*

6. Conclusions

This study was initiated as a consequence of an increasing concern about the fact that some CM-SAF products (including several of the cloud products) are depending on input provided by NWP models. Since one of the objectives of the CM-SAF is to provide independent observation datasets suitable for use in model validation applications, it is important to prove that the CM-SAF datasets still can be considered as being "enough" independent even if some NWP information has been used as background information in the CM-SAF product generation.

As an overall conclusion from the results of the study, it can be stated that the NWP model influence on the results of the three cloud products cloud fractional cover, cloud type and cloud top height appears to be small. An interchange of NWP model analysis input data to the PPS cloud processing method, using data from the three NWP models HIRLAM, ECMWF and GME, did only lead to marginal changes of the resulting CM-SAF cloud products. Thus, the current CM-SAF cloud products should be able to show robust results that are not heavily dependent on NWP model background information (see also a further illustration in Appendix 1).

A major factor explaining the small influence is that CM-SAF is using model **analyses** and **not forecasts** (as a contrast to other satellite applications, e.g. such as those being run by the NWCSAF project). Thus, it is assumed that the input data is dominated by assimilated observations or measurements and therefore much less affected by contributions from model first guess information (usually short 6-hour forecasts) that primarily exist in areas where observations are scarce. It also means that the differences that are found are most probably related to differences in data assimilation methods or to differences in the used input observation data sets. One particularly important aspect here is the assimilation of ocean sea surface temperature (SST) information, ice cover and snow cover which typically differs between the models. It also means that any improvements of models (or corresponding re-analysis datasets) will also directly influence the quality of the CM-SAF products in a positive way.

Nevertheless, the study demonstrated a natural high sensitivity to one of the used NWP model parameters; the surface skin temperature. This parameter is crucial for the *a priori* determination of the top of atmosphere clear sky radiance which is used for defining the used thresholds for the infrared cloud tests of the PPS method. It was shown that a perturbation of the surface skin temperature of one K resulted in change of cloud cover of about 0.5-1 %. However, if perturbations were in the range 5-10 K the change in cloud cover increased to values between 1 to 2 % per degree. Important to notice is also that the sign of the perturbations and the associated effects on cloud amounts are always the same, i.e., a positive surface temperature perturbation leads to an increase in the resulting cloud amounts and vice versa. This can be understood by considering the fact that a negative perturbation is equivalent to increasing the safety margin (or the threshold offset value) for the cloud detection process. The safety margin is an important tuning parameter that must be optimised for minimising the risk of mistaking cloud-free surface pixels for being cloudy. Likewise, a positive perturbation is then equivalent to reducing the safety margin. Due to these circumstances, it is easily understood that the introduction of a positive perturbation is more serious than introducing a negative perturbation. For example, a perturbation of +10 K was shown to increase cloud amounts by about 20 % in absolute terms while the corresponding decrease in cloud amounts with a perturbation of -10 K was about 5 %. Thus, for the current PPS cloud detection scheme a positive bias in NWP surface temperatures is more serious for the results than a negative bias.

Concerning the effect on the cloud products Cloud Type and Cloud Top Height, the sensitivity study naturally affected almost exclusively the frequency of Low-level clouds and the associated frequency of pixels with low Cloud Top Heights. However, also the contributions from high clouds were slightly

changed (and in the opposite way compared to the Low-level clouds) since the perturbed surface temperatures changed the pre-calculated atmospheric corrections of the used thresholds for identification of semi-transparent Cirrus clouds.

What the study has not been able to address or further elaborate on is the following fundamental question:

- Why do we really need to use NWP background information for managing the cloud parameter retrieval task?

The results of this study (at least the NWP model inter-comparison part) could potentially be misinterpreted as suggesting that the NWP model background information does not contribute to improving CM-SAF results. Such an interpretation is unfortunate and in many aspects incorrect. For example, for the cloud top height and cloud type interpretation access to NWP analysed atmospheric profiles is essential. However, for other products (like Cloud Fractional Cover) the situation is more unclear. What remains to be proven is that, even if we are not seriously dependent on NWP background information (i.e., errors or variations in NWP model input are not very serious for the quality of CM-SAF results), the access of this information is nevertheless considerably improving the quality of CM-SAF products, and more specifically, the fundamental cloud detection task.

This aspect will be studied further in the CM-SAF. The problem can be formulated more clearly by the following:

- Are CM-SAF CFC products significantly improved if using dynamical thresholds (utilising the best possible information on the atmospheric state at the time of the satellite measurement) in comparison with traditional static thresholding approaches (using fixed thresholds determined from an analysis of longer periods with data – weeks or months)?

It is hoped that the results of the current study can be later complemented with corresponding results using static surface and moisture datasets (e.g. climatologies from Re-analysis efforts). This could help answering the two fundamental questions above. More concretely, such a complementary study accompanied also with some validation efforts (comparisons with real cloud observations) could show if the CM-SAF approach is better than other climate monitoring approaches using constant cloud analysis thresholds over longer periods (e.g., the ISCCP methodology).


Acknowledgements

Appendix 1 – Illustrating the robustness of CM-SAF cloud detection: The impact of a serious GME grid orientation error

During the preparation of the model inter-comparison part of this study (presented in Section 5), a serious error in the configuration of the PPS NWP interface to the GME model occurred. The error lead to an incorrect indexing of latitude and longitude information and eventually to that the mapped model grid field was turned upside down. Thus, the result was that all the datasets from GME was extracted from a position on the other side of the Earth! More clearly, the presumed information over the Baltrad1km area (Figure 1) was instead fetched from a position in the southern part of the Pacific Ocean close to the Antarctic continent.

The result of this seemingly brutal and dramatic error in PPS input data is seen in the figure below which is the same plot as in the previous Figure 10 in Section 4 but now after having used the incorrectly configured PPS version. We notice that for large parts of the year GME results are not drastically different despite being based on completely incorrect GME model information. However, there are two specific periods during which results based on GME data are now deviating significantly (summer and winter). Maximum deviations are found for August 2004 (+11 %) and for February-March 2005 (+8 %). This is logical in the sense that it is in these seasons we should expect the largest surface temperature differences between the studied region and the corresponding misprojected region (i.e., the region in the southern Pacific Ocean close to the Antarctic). For the spring and autumn seasons temperature differences are much smaller and, consequently, the impact on PPS results is much smaller.

We can easily understand the large positive deviations in the northern Scandinavian winter. It is clear that during winter we will use too warm surface temperatures in this region and this will lead to overestimated cloud amounts (as concluded in the previous Section 3). It is more complicated to understand the corresponding overestimation of cloudiness for the northern Scandinavian summer period (i.e., according to conclusions in Section 3 an underestimation of surface temperatures should lead to a decrease in cloud amounts). However, if we consider that the map error actually means that we by mistake will use surface temperature information representative for ice cover close to the Antarctic continent (often as cold as -30 °C) instead of typical summer temperatures ($\approx$ +20 °C) we realise that the encountered cloud processing conditions are very extreme (i.e., assuming Arctic or Antarctic conditions during northern hemisphere summer!) compared to the cases previously explored in Section 3. Obviously, the selection or preparation of PPS thresholds for the basic cloud detection process fails completely in this extreme case. This was further enhanced by some PPS weaknesses in the pre-calculated threshold information for very cold conditions (which will be removed in the next PPS version released in 2008) and a large overestimation of summertime cloudiness occurred as a result.

In conclusion, we have seen that a very drastic and serious error in the input NWP model information to PPS actually led to rather limited error in the derived cloud information. Thus, the sensitivity to the background NWP model information is relatively weak.
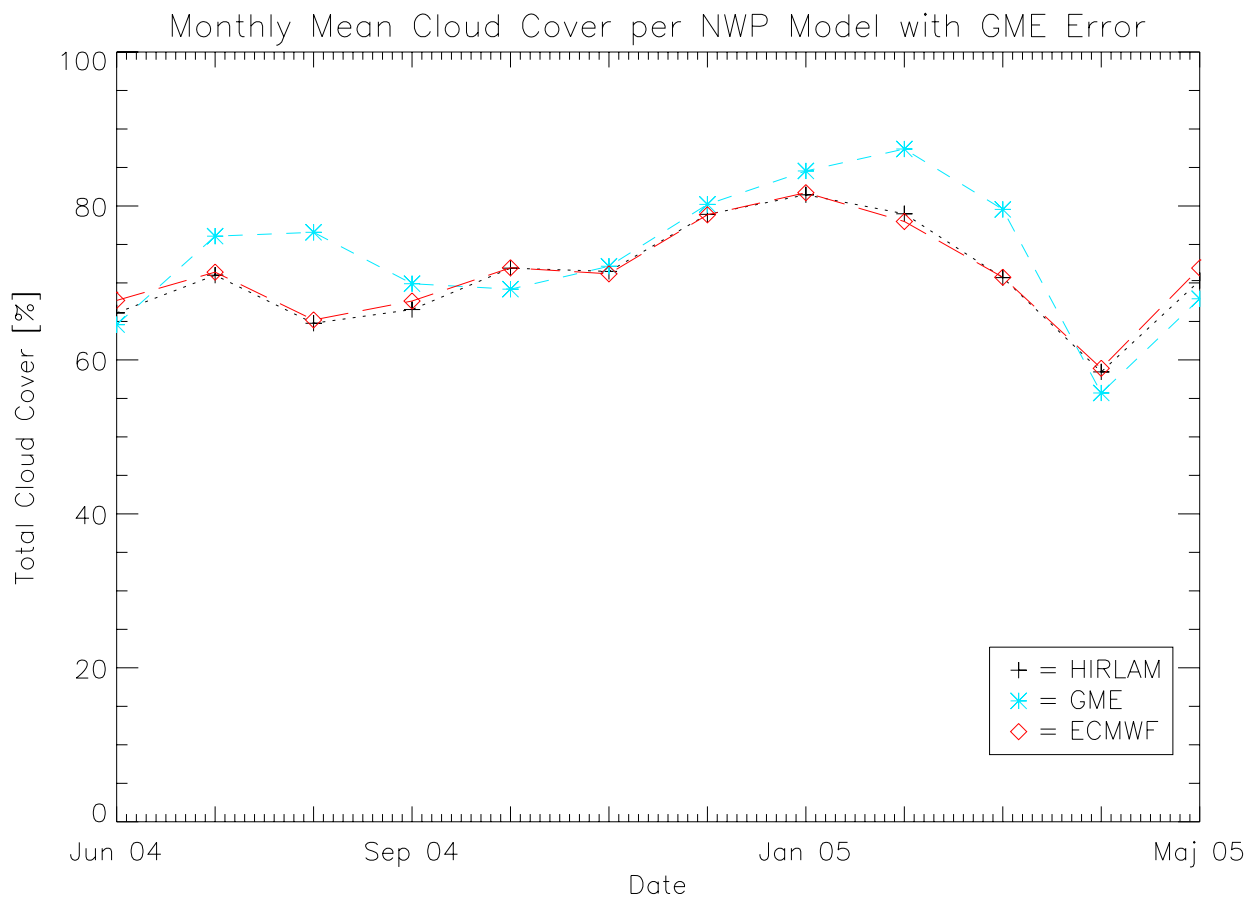
Time-series of PPS-derived monthly mean cloud cover over the Baltrad1km are for each NWP model used as background information for the PPS cloud software. **Observe:** *In this figure the GME results are incorrect due to a serious grid orientation error (see text).*

Acronyms

AAPP	ATOVS and AVHRR Pre-processing Package
AVHRR	Advanced Very High Resolution Radiometer
ATOVS	Advanced Tiros Operational Vertical Sounder (on polar NOAA satellites and on MetOp)
CDOP	Continued Development and Operations Phase (EUMETSAT SAFs)
CM-SAF	Climate Monitoring Satellite Application Facility project (EUMETSAT)
DWD	Deutscher Wetterdienst (German Weather Service)
ECMWF	European Centre for Medium-range Weather Forecasts (Reading, UK)
EUMETSAT	European organisation for exploitation of meteorological satellites
ISCCP	International Satellite Cloud Climatology Project (WMO-WCRP)
NOAA	National Oceanographic and Atmospheric Administration (USA)
NWCSAF	Satellite Application Facility in support of Nowcasting and Short-range Forecasting applications (EUMETSAT)
NWP	Numerical Weather Prediction
PPS	The Polar Platform System cloud processing software (NWCSAF)
RTM	Radiative Transfer Model
RTTOV	Radiative Transfer for TOVS (RTM model from NWPSAF)
SEVIRI	Spinning Enhanced Visible and Infrared radiometer (on Meteosat Second Generation satellites, EUMETSAT)
SMHI	The Swedish Meteorological and Hydrological Institute
SST	Sea Surface Temperature
TOA	Top of Atmosphere

References

Dybbroe A. and P. Hultgren 2000: The SMHI database Matching Satellite, Model and Synop data - User's manual.

Dybbroe, R., K.-G. Karlsson and A. Thoss, 2005a: NWCSAF AVHRR cloud detection and analysis using dynamic thresholds and radiative transfer modelling. Part I: Algorithm description. *J. Appl. Meteor.,* **44**, 39-54.

Dybbroe, R., K.-G. Karlsson and A. Thoss, 2005b: NWCSAF AVHRR cloud detection and analysis using dynamic thresholds and radiative transfer modelling. Part II: Validation and tuning. *J. Appl. Meteor.,* **44**, 55-71.

Korpela, A., A. Dybbroe and A. Thoss, 2001: Retrieving Cloud Top Temperature and Height in Semi-transparent and Fractional Cloudiness using AVHRR, NWCSAF Visiting Scientist Report, SMHI/NIWA, October 2001, 48 pp.

NWCSAF SUM, 2008: *Scientific User Manual for the AVHRR/AMSU cloud and precipitation product of the SAFNWC/PPS.*

Saunders, R.W., M. Matricardi and P. Brunel, 1999: An improved fast radiative transfer model for assimilation of satellite radiances observations, *Quart. J. Roy. Meteor. Soc.,* **125**, 1407-1425.

Undén et. al, 2002: HIRLAM-5 Scientific Documentation. HIRLAM-5 Project.

SMHIs publiceringar

SMHI ger ut sex rapportserier. Tre av dessa, R-serierna är avsedda för internationell publik och skrivs därför oftast på engelska. I de övriga serierna används det svenska språket.

Seriernas namn	Publiceras sedan
RMK (Rapport Meteorologi och Klimatologi)	1974
RH (Rapport Hydrologi)	1990
RO (Rapport Oceanografi)	1986
METEOROLOGI	1985
HYDROLOGI	1985
OCEANOGRAFI	1985

I serien METEOROLOGI har tidigare utgivits:

1985
1 Hagmarker, A. (1985)
   Satellitmeteorologi.

2 Fredriksson, U., Persson, Ch., Laurin, S. (1985)
   Helsingborgsluft.

3 Persson, Ch., Wern, L. (1985)
   Spridnings- och depositionsberäkningar för av fallsförbränningsanläggningar i Sofielund och Högdalen.

4 Kindell, S. (1985)
   Spridningsberäkningar för SUPRAs anläggningar i Köping.

5 Andersson, C., Kvick, T. (1985)
   Vindmätningar på tre platser på Gotland. Utvärdering nr 1.

6 Kindell, S. (1985)
   Spridningsberäkningar för Ericsson, Ingelstafabriken.

7 Fredriksson, U. (1985)
   Spridningsberäkningar för olika plymlyft vid avfallsvärmeverket Sävenäs.

8 Fredriksson, U., Persson, Ch. (1985)
   NO_x- och NO_2-beräkningar vid Vasaterminalen i Stockholm.

9 Wern, L. (1985)
   Spridningsberäkningar för ASEA transformers i Ludvika.

10 Axelsson, G., Eklind, R. (1985)
    Ovädret på Östersjön 23 juli 1985.

11 Laurin, S., Bringfelt, B. (1985)
    Spridningsmodell för kväveoxider i gatumiljö.

12 Persson, Ch., Wern, L. (1985)
    Spridnings- och depositionsberäkningar för avfallsförbränningsanläggning i Sofielund.

13 Persson, Ch., Wern, L. (1985)
    Spridnings- och depositionsberäkningar för avfallsförbränningsanläggning i Högdalen.

14 Vedin, H., Andersson, C. (1985)
    Extrema köldperioder i Stockholm.

15 Krieg, R., Omstedt, G. (1985)
    Spridningsberäkningar för Volvos planerade bilfabrik i Uddevalla.

16 Kindell, S. Wern, L. (1985)
    Luftvårdsstudie avseende industrikombinatet i Nynäshamn (koncentrations- och luktberäkningar).

17 Laurin, S., Persson, Ch. (1985)
    Beräknad formaldehydspridning och deposition från SWEDSPANs spånskivefabrik.

18 Persson, Ch., Wern, L. (1985)
    Luftvårdsstudie avseende industri-kombinatet i Nynäshamn – depositions-beräkningar av koldamm.

19 Fredriksson, U. (1985)
Luktberäkningar för Bofors Plast i
Ljungby, II.

20 Wern, L., Omstedt, G. (1985)
Spridningsberäkningar för Volvos
planerade bilfabrik i Uddevalla - energi-
centralen.

21 Krieg, R., Omstedt, G. (1985)
Spridningsberäkningar för Volvos
planerade bilfabrik i Uddevalla -
kompletterande beräkningar för fabrikerna.

22 Karlsson, K.-G. (1985)
Information från Meteosat - forskningsrön
och operationell tillämpning.

23 Fredriksson, U. (1985)
Spridningsberäkningar för AB Åkerlund &
Rausings fabrik i Lund.

24 Färnlöf, S. (1985)
Radarmeteorologi.

25 Ahlström, B., Salomonsson, G. (1985)
Resultat av 5-dygnsprognos till ledning för
isbrytarverksamhet vintern 1984-85.

26 Wern, L. (1985)
Avesta stadsmodell.

27 Hultberg, H. (1985)
Statistisk prognos av yttemperatur.

1986

1 Krieg, R., Johansson, L., Andersson, C.
(1986)
Vindmätningar i höga master, kvartals-
rapport 3/1985.

2 Olsson, L.-E., Kindell, S. (1986)
Air pollution impact assessment for the
SABAH timber, pulp and paper complex.

3 Ivarsson, K.-I. (1986)
Resultat av byggväderprognoser -
säsongen 1984/85.

4 Persson, Ch., Robertson, L. (1986)
Spridnings- och depositionsberäkningar
för en sopförbränningsanläggning i
Skövde.

5 Laurin, S. (1986)
Bilavgaser vid intagsplan - Eskilstuna.

6 Robertson, L. (1986)
Koncentrations- och depositions-
beräkningar för en sopförbrännings-
anläggning vid Ryaverken i Borås.

7 Laurin, S. (1986)
Luften i Avesta - föroreningsbidrag från
trafiken.

8 Robertson, L., Ring, S. (1986)
Spridningsberäkningar för bromcyan.

9 Wern, L. (1986)
Extrema byvindar i Orrefors.

10 Robertson, L. (1986)
Koncentrations- och depositions-
beräkningar för Halmstads avfalls-
förbränningsanläggning vid Kristinehed.

11 Törnevik, H., Ugnell (1986)
Belastningsprognoser.

12 Joelsson, R. (1986)
Något om användningen av numeriska
prognoser på SMHI (i princip rapporten
till ECMWF).

13 Krieg, R., Andersson, C. (1986)
Vindmätningar i höga master, kvartals-
rapport 4/1985.

14 Dahlgren, L. (1986)
Solmätning vid SMHI.

15 Wern, L. (1986)
Spridningsberäkningar för ett kraftvärme-
verk i Sundbyberg.

16 Kindell, S. (1986)
Spridningsberäkningar för Uddevallas
fjärrvärmecentral i Hovhult.

17 Häggkvist, K., Persson, Ch., Robertson, L
(1986)
Spridningsberäkningar rörande gasutsläpp
från ett antal källor inom SSAB Luleå-
verken.

18 Krieg, R., Wern, L. (1986)
En klimatstudie för Arlanda stad.

19 Vedin, H. (1986)
Extrem arealnederbörd i Sverige.

20 Wern, L. (1986)
Spridningsberäkningar för lösningsmedel i
Tibro.

21 Krieg, R., Andersson, C. (1986)
Vindmätningar i höga master - kvartals-
rapport 1/1986.

22 Kvick, T. (1986)
Beräkning av vindenergitillgången på
några platser i Halland och Bohuslän.

23 Krieg, R., Andersson, C. (1986)
Vindmätningar i höga master - kvartals-
rapport 2/1986.

24 Persson, Ch. (SMHI), Rodhe, H.
(MISU), De Geer, L.-E. (FOA) (1986)
Tjernobylolyckan - En meteorologisk
analys av hur radioaktivitet spreds till
Sverige.

25 Fredriksson, U. (1986)
Spridningsberäkningar för Spendrups
bryggeri, Grängesberg.

26 Krieg, R. (1986)
Beräkningar av vindenergitillgången på
några platser i Skåne.

27 Wern, L., Ring, S. (1986)
Spridningsberäkningar, SSAB.

28 Wern, L., Ring, S. (1986)
Spridningsberäkningar för ny ugn,
SSAB II.

29 Wern, L. (1986)
Spridningsberäkningar för Volvo
Hallsbergverken.

30 Fredriksson, U. (1986)
SO_2-halter från Hammarbyverket kring ny
arena vid Johanneshov.

31 Persson, Ch., Robertson, L., Häggkvist, K.
(1986)
Spridningsberäkningar, SSAB - Luleå-
verken.

32 Kindell, S., Ring, S. (1986)
Spridningsberäkningar för SAABs
planerade bilfabrik i Malmö.

33 Wern, L. (1986)
Spridningsberäkningar för
svavelsyrafabrik i Falun.

34 Wern, L., Ring, S. (1986)
Spridningsberäkningar för Västhamns-
verket HKV1 i Helsingborg.

35 Persson, Ch., Wern, L. (1986)
Beräkningar av svaveldepositionen i
Stockholmsområdet.

36 Joelsson, R. (1986)
USAs månadsprognoser.

37 Vakant nr.

38 Krieg, R., Andersson, C. (1986)
Utemiljön vid Kvarnberget, Lysekil.

39 Häggkvist, K. (1986)
Spridningsberäkningar av freon 22 från
Ropstens värmepumpverk.

40 Fredriksson, U. (1986)
Vindklassificering av en plats på Hemsön.

41 Nilsson, S. (1986)
Utvärdering av sommarens (1986)
använda konvektionsprognoshjälpmedel.

42 Krieg, R., Kvick, T. (1986)
Vindmätningar i höga master.

43 Krieg, R., Fredriksson, U. (1986)
Vindarna över Sverige.

44 Robertson, L. (1986)
Spridningsberäkningar rörande gasutsläpp
vid ScanDust i Landskrona - bestämning
av cyanvätehalter.

45 Kvick, T., Krieg, R., Robertson, L. (1986)
Vindförhållandena i Sveriges kust- och
havsband, rapport nr 2.

46 Fredriksson, U. (1986)
Spridningsberäkningar för en planerad
panncentral vid Lindsdal utanför Kalmar.

47 Fredriksson, U. (1986)
Spridningsberäkningar för Volvo BMs
fabrik i Landskrona.

48 Fredriksson, U. (1986)
Spridningsberäkningar för ELMO-CALFs
fabrik i Svenljunga.

49 Häggkvist, K. (1986)
Spridningsberäkningar rörande gasutsläpp
från syrgas- och bensenupplag inom SSAB
Luleåverken.

50 Wern, L., Fredriksson, U., Ring, S. (1986)
Spridningsberäkningar för lösningsmedel i
Tidaholm.

51 Wern, L. (1986)
Spridningsberäkningar för Volvo BM ABs
anläggning i Braås.

52 Ericson, K. (1986)
Meteorological measurements performed
May 15, 1984, to June, 1984, by the
SMHI.

53 Wern, L., Fredriksson, U. (1986)
Spridningsberäkning för Kockums Plåt-
teknik, Ronneby.

54 Eriksson, B. (1986)
Frekvensanalys av timvisa temperatur-
observationer.

55 Wern, L., Kindell, S. (1986)
Luktberäkningar för AB ELMO i Flen.

56 Robertson, L. (1986)
Spridningsberäkningar rörande utsläpp av
NO_x inom Fagersta kommun.

57 Kindell, S. (1987)
Luften i Nässjö.

58 Persson, Ch., Robertson, L. (1987)
Spridningsberäkningar rörande gasutsläpp
vid ScanDust i Landskrona - bestämning
av cyanväte.

59 Bringfelt, B. (1987)
Receptorbaserad partikelmodell för
gatumiljömodell för en gata i Nyköping.

60 Robertson, L. (1987)
Spridningsberäkningar för Varbergs
kommun. Bestämning av halter av SO_2,
CO, NO_x samt några kolväten.

61 Vedin, H., Andersson, C. (1987)
E 66 - Linderödsåsen - klimatförhållanden.

62 Wern, L., Fredriksson, U. (1987)
Spridningsberäkningar för Kockums
Plåtteknik, Ronneby. 2.

63 Taesler, R., Andersson, C., Wallentin, C.,
Krieg, R. (1987)
Klimatkorrigering för energiförbrukningen
i ett eluppvärmt villaområde.

64 Fredriksson, U. (1987)
Spridningsberäkningar för AB Åetå-
Trycks planerade anläggning vid Kungens
Kurva.

65 Melgarejo, J. (1987)
Mesoskalig modellering vid SMHI.

66 Häggkvist, K. (1987)
Vindlaster på kordahus vid Alviks Strand -
numeriska beräkningar.

67 Persson, Ch. (1987)
Beräkning av lukt och föroreningshalter i
luft runt Neste Polyester i Nol.

68 Fredriksson, U., Krieg, R. (1987)
En överskalig klimatstudie för Tornby,
Linköping.

69 Häggkvist, K. (1987)
En numerisk modell för beräkning av
vertikal momentumtransport i områden
med stora råhetselement. Tillämpning på
ett energiskogsområde.

70 Lindström, Kjell (1987)
Weather and flying briefing aspects.

71 Häggkvist, K. (1987)
En numerisk modell för beräkning av
vertikal momentumtransport i områden
med stora råhetselement. En koefficient-
bestämning.

72 Liljas, E. (1988)
Förbättrad väderinformation i jordbruket -
behov och möjligheter (PROFARM).

73 Andersson, Tage (1988)
Isbildning på flygplan.

74 Andersson, Tage (1988)
Aeronautic wind shear and turbulence.
A review for forecasts.

75 Kållberg, P. (1988)
Parameterisering av diabatiska processer i
numeriska prognosmodeller.

76 Vedin, H., Eriksson, B. (1988)
Extrem arealnederbörd i Sverige
1881 - 1988.

77 Eriksson, B., Carlsson, B., Dahlström, B.
(1989)
Preliminär handledning för korrektion av
nederbördsmängder.

78 Liljas, E. (1989)
Torv-väder. Behovsanalys med avseende
på väderprognoser och produktion av
bränsletorv.

79 Hagmarker, A. (1991)
Satellitmeteorologi.

80 Lövblad, G., Persson, Ch. (1991)
Background report on air pollution
situation in the Baltic states - a
prefeasibility study.
IVL Publikation B 1038.

81 Alexandersson, H., Karlström, C.,
Larsson-McCann, S. (1991)
Temperaturen och nederbörden i Sverige
1961-90. Referensnormaler.

82   Vedin, H., Alexandersson, H., Persson, M. (1991)
Utnyttjande av persistens i temperatur och nederbörd för vårflödesprognoser.

83   Moberg, A. (1992)
Lufttemperaturen i Stockholm 1756 - 1990. Historik, inhomogeniteter och urbaniseringseffekt.
Naturgeografiska Institutionen, Stockholms Universitet.

84   Josefsson, W. (1993)
Normalvärden för perioden 1961-90 av globalstrålning och solskenstid i Sverige.

85   Laurin, S., Alexandersson, H. (1994)
Några huvuddrag i det svenska temperatur-klimatet 1961 - 1990.

86   Fredriksson, U. och Ståhl, S. (1994)
En jämförelse mellan automatiska och manuella fältmätningar av temperatur och nederbörd.

87   Alexandersson, H., Eggertsson Karlström, C. och Laurin S. (1997).
Några huvuddrag i det svenska nederbördsklimatet 1961-1990.

88   Mattsson, J., Rummukainen, M. (1998)
Växthuseffekten och klimatet i Norden - en översikt.

89   Kindbom, K., Sjöberg, K., Munthe, J., Peterson, K. (IVL)
Persson, C. Roos, E., Bergström, R. (SMHI). (1998)
Nationell miljöövervakning av luft- och nederbördskemi 1996.

90   Foltescu, V.L., Häggmark, L (1998)
Jämförelse mellan observationer och fält med griddad klimatologisk information.

91   Hultgren, P., Dybbroe, A., Karlsson, K.-G. (1999)
SCANDIA – its accuracy in classifying LOW CLOUDS

92   Hyvarinen, O., Karlsson, K.-G., Dybbroe, A. (1999)
Investigations of NOAA AVHRR/3 1.6 μm imagery for snow, cloud and sunglint discrimination (Nowcasting SAF)

93   Bennartz, R., Thoss, A., Dybbroe, A. and Michelson, D. B. (1999)
Precipitation Analysis from AMSU (Nowcasting SAF)

94   Appelqvist, Peter och Anders Karlsson (1999)
Nationell emissionsdatabas för utsläpp till luft - Förstudie.

95   Persson, Ch., Robertson L. (SMHI) Thaning, L (LFOA). (2000)
Model for Simulation of Air and Ground Contamination Associated with Nuclear Weapons. An Emergency Preparedness Model.

96   Kindbom K., Svensson A., Sjöberg K., (IVL) Persson C., (SMHI) (2001)
Nationell miljöövervakning av luft- och nederbördskemi 1997, 1998 och 1999.

97   Diamandi, A., Dybbroe, A. (2001)
Nowcasting SAF
Validation of AVHRR cloud products.

98   Foltescu V. L., Persson Ch. (2001)
Beräkningar av moln- och dimdeposition i Sverigemodellen - Resultat för 1997 och 1998.

99   Alexandersson, H. och Eggertsson Karlström, C (2001)
Temperaturen och nederbörden i Sverige 1961-1990. Referensnormaler - utgåva 2.

100   Korpela, A., Dybbroe, A., Thoss, A. (2001)
Nowcasting SAF - Retrieving Cloud Top Temperature and Height in Semi-transparent and Fractional Cloudiness using AVHRR.

101   Josefsson, W. (1989)
Computed global radiation using interpolated, gridded cloudiness from the MESA-BETA analysis compared to measured global radiation.

102   Foltescu, V., Gidhagen, L., Omstedt, G. (2001)
Nomogram för uppskattning av halter av PM_{10} och NO_2

103   Omstedt, G., Gidhagen, L., Langner, J. (2002)
Spridning av förbränningsemissioner från småskalig biobränsleeldning
– analys av PM2.5 data från Lycksele med hjälp av två Gaussiska spridningsmodeller.

104   Alexandersson, H. (2002)
Temperatur och nederbörd i Sverige 1860 - 2001

105   Persson, Ch. (2002)
Kvaliteten hos nederbördskemiska mätdata

som utnyttjas för dataassimilation i MATCH-Sverige modellen".

106 Mattsson, J., Karlsson, K-G. (2002)
CM-SAF cloud products feasibility study in the inner Arctic region
Part I: Cloud mask studies during the 2001 Oden Arctic expedition

107 Kärner, O., Karlsson, K-G. (2003)
Climate Monitoring SAF - Cloud products feasibility study in the inner Arctic region.
Part II: Evaluation of the variability in radiation and cloud data

108 Persson, Ch., Magnusson, M. (2003)
Kvaliteten i uppmätta nederbördsmängder inom svenska nederbörskemiska stationsnät

109 Omstedt, G., Persson Ch., Skagerström, M (2003)
Vedeldning i småhusområden

110 Alexandersson, H., Vedin, H. (2003)
Dimensionerande regn för mycket små avrinningsområden

111 Alexandersson, H. (2003)
Korrektion av nederbörd enligt enkel klimatologisk metodik

112 Joro, S., Dybbroe, A.(2004)
Nowcasting SAF – IOP
Validating the AVHRR Cloud Top Temperature and Height product using weather radar data
Visiting Scientist report

113 Persson, Ch., Ressner, E., Klein, T. (2004)
Nationell miljöövervakning – MATCH-Sverige modellen
Metod- och resultatsammanställning för åren 1999-2002 samt diskussion av osäkerheter, trender och miljömål

114 Josefsson, W. (2004)
UV-radiation measured in Norrköping 1983-2003.

115 Martin, Judit, (2004)
Var tredje timme – Livet som väderobservatör

116 Gidhagen, L., Johansson, C., Törnquist, L. (2004)
NORDIC – A database for evaluation of dispersion models on the local, urban and regional scale

117 Langner, J., Bergström, R., Klein, T., Skagerström, M. (2004)

Nuläge och scenarier för inverkan på marknära ozon av emissioner från Västra Götalands län – Beräkningar för 1999

118 Trolez, M., Tetzlaff, A., Karlsson, K-G. (2005)
CM-SAF Validating the Cloud Top Height product using LIDAR data

119 Rummukainen, M. (2005)
Växthuseffekten

120 Omstedt, G. (2006)
Utvärdering av PM_{10} mätningar i några olika nordiska trafikmiljöer

121 Alexandersson, H. (2006)
Vindstatistik för Sverige 1961-2004

122 Samuelsson, P., Gollvik, S., Ullerstig, A., (2006)
The land-surface scheme of the Rossby Centre regional atmospheric climate model (RCA3)

123 Omstedt, G. (2007)
VEDAIR – ett internetverktyg för beräkning av luftkvalitet vid småskalig biobränsleeldning
Modellbeskrivning och slutrapport mars 2007

124 Persson, G., Strandberg, G., Bärring, L., Kjellström, E. (2007)
Beräknade temperaturförhållanden för tre platser i Sverige – perioderna 1961-1990 och 2011-2040

125 Engart, M., Foltescu, V. (2007)
Luftföroreningar i Europa under framtida klimat

126 Jansson, A., Josefsson, W. (2007)
Modelling of surface global radiation and CIE-weighted UV-radiation for the period 1980-2000

127 Johnston, S., Karlsson, K-G. (2007)
METEOSAT 8 SEVIRI and NOAA Cloud Products. A Climate Monitoring SAF Comparison Study

128 Eliasson, S., Tetzlaf, A., Karlsson, K-G. (2007)
Prototyping an improved PPS cloud detection for the Arctic polar night

SMHI